Journal of Sustainable Development of Energy, Water and Environment Systems

http://www.sdewes.org/jsdewes

Year 2027, Volume 15, Issue 1, 1140773

Original Research Article

Prevention of corrosion and scale formation problems in water systems at 50°C by isobutylamide derivatives of ethylenediaminetetraacetic acid

Teyyub A. Ismayilov[1], Rahima M. Farhadova[1], Ismayil T. Ismayilov[1], Vagif M. Abbasov[1], Ayaz M. Mammadov[1,2,3], Sara M. Abbaszade[1], Elmir A. Manafov[4], Gunel T. Aghamaliyeva[1]

[1]Institute of Petrochemical Processes named after academician Y.H. Mammadaliyev of the Ministry of Science and Education of the Republic of Azerbaijan, AZ1025, Khojaly ave. 30, Baku, Azerbaijan
e-mail: nkpi@nkpi.az

[2]Sumgait State University, Department of Chemistry, AZ5008, Baku Str. 1, Sumgait, Azerbaijan
e-mail: ayaz.mamedov@sdu.edu.az

[3]Azerbaijan University of Architecture and Construction, AZ1073, Ayna Sultanova Str. 5, Baku, Azerbaijan
e-mail: ayaz.mammadov1@azmiu.edu.az

[4]SEK International School Riyadh, 13315, Al Toq Str., Ar Rabi, Riyadh Saudi Arabia
e-mail: elmir.manafov@sek.sa

Cite as: Ismayilov, T. A., Farhadova, R. M., Ismayilov, I. T., Abbasov, V. M., Mammadov, A. M., Abbaszade, S. M., Manafov, E. A., Aghamaliyeva, G. T., Prevention of corrosion and scale formation problems in water systems at 50oC by isobutylamide derivatives of ethylenediaminetetraacetic acid, J.sustain. dev. energy water environ. syst., 15(1), 1140773, 2027, DOI: https://doi.org/10.13044/j.sdewes.d14.0773

Abstract

The article identifies the minerals that cause salt deposition in various industrial sectors and provides information on reagents used to prevent the salt deposition process, emphasizing a preference for those reagents that are multifunctional, environmentally friendly and economically viable. Sodium and potassium salts of mono-, di-, and triisobutylamides of ethylenediaminetetraacetic acid were synthesised for testing as corrosion and scale-forming inhibitors in water systems at 50°C. The structures of the synthesised compounds were confirmed by Infrared spectroscopy, and their 10% solutions were prepared to determine the main physicochemical parameters. Inhibition of corrosion and salt deposition experiments were carried out at concentrations of 50, 100 and 150 mg/L. At an amount of 50 mg/L, the trisodium salt of the amide synthesised from ethylenediaminetetraacetic acid and isobutylamine at a 1:1 molar ratio exhibited the highest performance, providing 90% protection of the Steel-3 metal plates against corrosion and achieving 90% effectiveness against salt precipitation. Anti-corrosion and anti-scaling evaluations showed that increasing the salt concentration to 100 and 150 mg/L led to a proportional increase in effectiveness. Analysis of the results also indicated that the mono-, di-, and trisodium salts demonstrated higher inhibitory properties compared to the corresponding potassium salts. In terms of activity, both the sodium and potassium salts followed the order: mono-<di-<tri-. It has been established that the inhibition mechanism of steel corrosion in the presence of synthesized salts is due to chemisorption, following the classical Langmuir adsorption isotherm. Additionally, computational calculations were performed to correlate the electronic properties of the inhibitors with their experimental performance, identifying the carboxylate and amide groups as the primary active centers for adsorption. The theoretical results, including frontier molecular energy level analysis and electron transfer fractions, provided a convincing explanation for the superior efficiency of the trisodium salt, consistent with the experimentally observed activity order of mono-<di-<tri-.

Keywords

water systems, scale prevention, corrosion inhibition, ethylenediaminetetraacetic acid, isobutylamide, corrosion and salt deposition reagent

Introduction

Water, which is widely used in households, also plays a very important role in industry. The total volume of water consumed worldwide is increasing every day. The use of water in various industrial sectors, including mining, the transportation of raw materials through pipelines, heating and cooling systems, and the preparation of solutions, is well established. During the use of water in the mentioned systems, various processes, corrosion [1], salt deposition [2], biomass formation [3], may occur over time, leading to problems such as reduced liquid flow rates [4], disruption of technological regimes and operational efficiency, premature equipment failure, and consequently increased costs [5].

Mechanical and chemical cleaning of the system, requiring interruption of the technological process, should also be regarded as a factor contributing to increased operational costs [6]. Methods of removing scale and corrosion deposits generally include mechanical, hydrodynamic, chemical, and electro-pulse cleaning techniques. Among these, the use of chemical reagents [7] is the most universal approach, as it is applied both to prevent the formation of corrosion and salt deposits [8], and to clean systems by dissolving existing deposits [9]. Thus, to avoid such problems, industrial enterprises apply corrosion and salt deposition inhibitors to mitigate corrosion and scaling, as well as biocides to prevent biomass formation, as part of preventive measures.

Some reagents are known to perform several functions simultaneously, and their use is therefore more economically efficient. It is possible to cite examples that have demonstrated high effectiveness as a carbon dioxide (CO_2) corrosion inhibitor and oil-collecting agent [10], a scale inhibitor and antibacterial agent [11], a corrosion inhibitor and biocide [12], and as a corrosion inhibitor in various aggressive environments [13].

Nowadays, increasing attention is paid to developing multifunctional reagents, preferably synthesised based on natural, renewable, and environmentally friendly raw materials. Paper [14] reviews recent research on the application of biomaterials as scale inhibitors in recirculating cooling water treatment systems. The study discusses various categories of environmentally friendly inhibitors, including proteins and amino acids, polysaccharides, plant extracts, microbial reagents, and microbiological products. In publication [15], the authors investigated a by-product of white oil production and evaluated its potential as an inhibitor-bactericidal reagent. In research work [16], several novel green surfactants derived from cottonseed oil were synthesized and tested as corrosion inhibitors for mild steel in a CO_2-saturated 1% sodium chloride solution using potentiodynamic polarization and linear polarization resistance measurements at 50°C. Similarly, article [17] investigated the adsorption behavior and corrosion inhibition performance of a series of commercial fatty acid surfactants synthesized from vegetable oils, including sunflower, cottonseed, corn, and palm oils, on mild steel in CO_2-saturated brine at 50°C. Research paper [18] reports the results of a study on green chemicals aimed at addressing corrosion, scaling, and microbial growth in open recirculating cooling water systems. The proposed all-organic multicomponent inhibitor blend, consisting of citric acid, phosphonates (hydroxyethylidene diphosphonic acid), an acrylate copolymer, and isothiazolone, demonstrated effective reduction of corrosion, scale deposition, and microbial growth under the tested conditions. Furthermore, the review article [19] provides a comprehensive overview of scale formation, various green scale inhibitors, their classifications, mechanisms of action, comparative performance, significance, and future prospects, offering valuable insights for researchers and professionals in the oil and gas industry.

These reagents can be single-component or multi-component compositions [20], [21], each performing an inhibitory function against one or more problems, such as corrosion, salt deposition, biomass formation, and biocorrosion. In this case, the effective composition of a reagent is determined through laboratory experiments and subsequently applied in industry [22]. To ensure the successful application of the reagent, technological parameters of the environment such as process temperature, flow rate, and the concentration of various minerals in the water as well as the material composition of equipment, should be considered [23].

The effectiveness of a salt-precipitation inhibitor is determined by the change in the total amount of calcium or salts in the environment. It is known that the main cause of scale formation is calcium carbonate ($CaCO_3$) present in water. In addition, minerals that contribute to salt precipitation include calcium sulphate, magnesium carbonate, magnesium sulphate, iron (II) carbonate, iron sulphide, barium and strontium sulphates [24].

One of the effective methods for treating mineral salt deposits is acid treatment of the medium. The first patent for this technology dates back to 1896 [25]. According to the patent, $CaCO_3$ reacts with hydrochloric acid during the acidification of the environment:

$$CaCO_3 + 2HCl = CaCl_2 + CO_2 + H_2O \quad (1)$$

Although it increased the efficiency of the system in which it was used fourfold, it did not gain widespread application owing to the severe corrosion it caused in equipment and technological devices. However, subsequent research led to the development of composite reagents that simultaneously prevent corrosion, which are still widely used today.

The literature includes studies on the effectiveness of organic complex compounds [25], phosphorus compounds [26], [27], nitrogen compounds [28], [29], low molecular weight polymers based on polyacrylate and polymaleic anhydride [30], [31], and surfactants [32] against corrosion and salt deposition. As noted in the article [25], according to many experts, acidic compositions prepared by adding chelate compounds to formulations are very effective against salt precipitation.

Zahraa and Falah [33] investigated the effectiveness of a corrosion inhibitor composition consisting of 100 ppm sodium benzoate, 60 ppm zinc sulfate, and ethylenediaminetetraacetic acid (EDTA) at concentrations of 10 and 20 ppm for carbon steel in saline environments at temperatures of 28, 33, and 38°C. The results demonstrated a significant reduction in corrosion rates upon the addition of the inhibitors and revealed a synergistic effect among the components in mitigating corrosion. While the binary inhibitor system (sodium benzoate + zinc sulfate) provided moderate protection, with efficiencies of up to 78%, the addition of EDTA significantly enhanced the inhibition efficiency, indicating a strong synergistic interaction when all three components were present. The highest inhibition efficiency, exceeding 99%, was achieved with 20 ppm EDTA at 33°C. It can be concluded that the combined action of anodic and cathodic inhibitors contributes to a reduction in the corrosion rate, while EDTA, acting as an anti-scaling agent, prevents the deposition of calcium and magnesium salts caused by temperature increases in heat exchangers.

Shaban et al. [34] and Brixi et al. [35] also investigated the combined effect of sodium benzoate and EDTA as corrosion inhibitors for carbon steel in chloride-containing solutions using electrochemical methods, with particular attention to the influence of temperature on inhibitor performance. The results demonstrated that the combined use of these inhibitors produced a synergistic effect, with inhibition efficiencies significantly higher than those achieved when each inhibitor was applied individually. The findings further indicated the formation of a strong protective film on the steel surface, which effectively reduced the corrosion rate.

Chelate compounds widely used as solvents of salt precipitation include diethylenetriaminepentaacetic acid [36], ethylenediaminetetraacetic acid [37], hydroxyethylethylenediaminetriacetic acid [38], 1-hydroxyethane-1, 1-diphosphonic acid [39], and their derivatives. These compounds form complexes with metal ions, preventing their

precipitation as salts, do not participate in active chemical reactions, are low in toxicity, have low corrosive activity, and are easy to transport and store.

EDTA is a chelating ligand with a high affinity constant and is capable of forming stable metal-EDTA complexes [40], [41]. Since the chelation reaction is stoichiometric, one mole of EDTA, for example, can bind two moles of calcium ions (Ca^{2+}) [42]. Also, due to its ability to form complexes with charged metal ions [43], EDTA has been extensively studied as a corrosion inhibitor for metals in various environments [44], [45]. Complexation occurs through interactions between the vacant d-orbitals of the metal and the free or π-electrons of EDTA, leading to the formation of donor-acceptor surface complexes [45]. It has been found that several parameters influence the inhibition efficiency of EDTA, including pH, temperature, concentration, and the type of metal.

Rehab and Kamal [46] investigated the corrosion inhibition performance of disodium EDTA salt for mild steel in Red Sea water using weight-loss measurements and electrochemical techniques. Their results demonstrated that disodium EDTA salt acts as an effective corrosion inhibitor, achieving an inhibition efficiency of approximately 88% for mild steel in Red Sea water. Furthermore, the inhibition efficiency increased with increasing disodium EDTA salt concentration and reaction temperature. In another study [47], Rehab tested the inhibitory effect of EDTA at very low concentrations on aluminium corrosion in 0.5 M hydrochloric acid solution. The calculated thermodynamic and adsorption parameters indicated that EDTA is chemisorbed onto the aluminium surface within this concentration range, forming a stable Al-EDTA complex. As a result, an inhibition efficiency of up to 89% was achieved.

The literature review indicates that EDTA and its derivatives exhibit effectiveness against both scale formation and corrosion, thereby performing multiple functions simultaneously. As mentioned earlier, the use of such reagents is considered economically advantageous, and research in this field is still under development.

The aim of the work presented in this article was to synthesize ethylenediaminetetraacetic acid mono-, di-, and tri-isobutyl amide derivatives and their corresponding sodium and potassium salts, to study the effectiveness of the synthesised compounds against corrosion and salt precipitation. Their activities as corrosion inhibitors in hydrogen sulphide environments and as bactericides against sulphate-reducing bacteria were evaluated [48], [49], yielding results that indicate the synthesised compounds may be regarded as multifunctional reagents.

Synthesis method of the isobutylamide derivatives of ethylenediaminetetraacetic acid

The synthesis of the sodium and potassium salts of mono-, di-, and triisobutylamides of ethylenediaminetetraacetic acid was carried out in two stages. In the first stage, mono-, di- and triisobutylamides of ethylenediaminetetraacetic acid were synthesised at temperatures of 120-150°C via the reaction of EDTA with isobutylamine at molar ratios ranging from 1:1 to 1:3. In the second stage, the corresponding mono-, di-, and trisodium and potassium salts were obtained by reacting the synthesised amides with 20% aqueous sodium hydroxide ($NaOH$) or potassium hydroxide (KOH) solutions. The synthesis reactions of the isobutylamides can be represented as follows:

$$(HOOCCH_2)_2NCH_2CH_2N(CH_2COOH)_2 + aNH_2CH_2CH(CH_3)CH_3 \longrightarrow$$
$$(HOOCCH_2)_{4-a}(NCH_2CH_2N)(CH_2COO^{-+}NH_3CH_2CH(CH_3)CH_3)_a \longrightarrow$$
$$(HOOCCH_2)_{4-a}(NCH_2CH_2N)(CH_2CONHCH_2CH(CH_3)CH_3)_a + aH_2O$$

where a = 1-3; the compound $(HOOCCH_2)_{4-a}(NCH_2CH_2N)(CH_2CONHCH_2CH(CH_3)CH_3)_a$ is the general formula for the isobutylamides.

When the synthesised isobutylamides are exposed to an alkaline solution, they undergo reactions that lead to the formation of salts. These reactions are schematically illustrated using mono-, di- and trisodium salts as examples.

Preparation of the trisodium salt of monoisobutylamide of ethylenediaminetetraacetic acid:

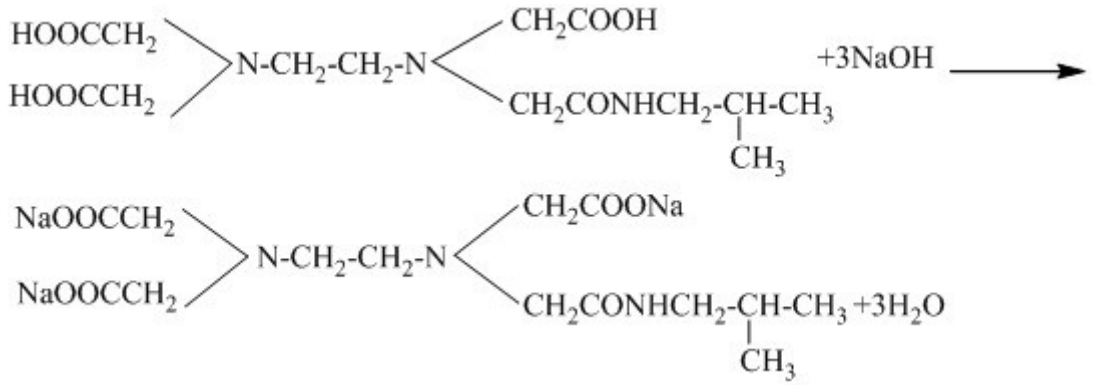

Preparation of the disodium salt of diisobutylamide of ethylenediaminetetraacetic acid:

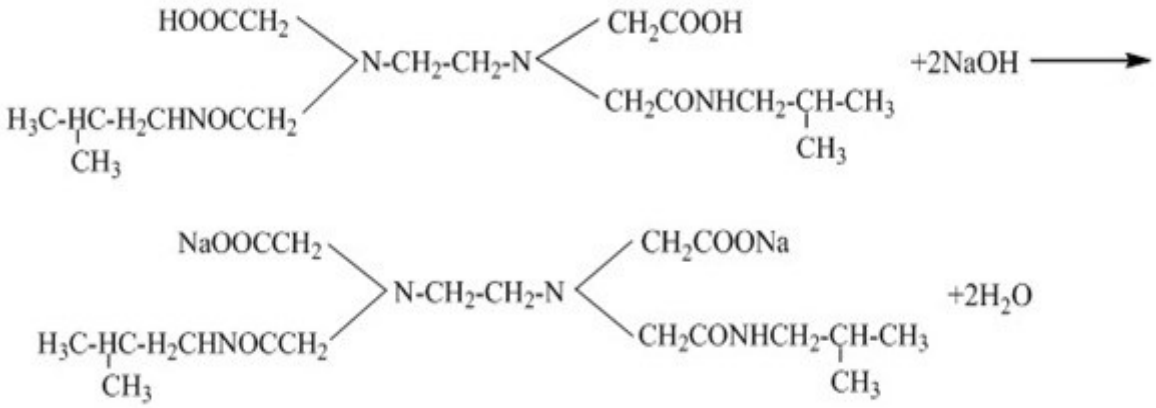

Preparation of the monosodium salt of triisobutylamide of ethylenediaminetetraacetic acid:

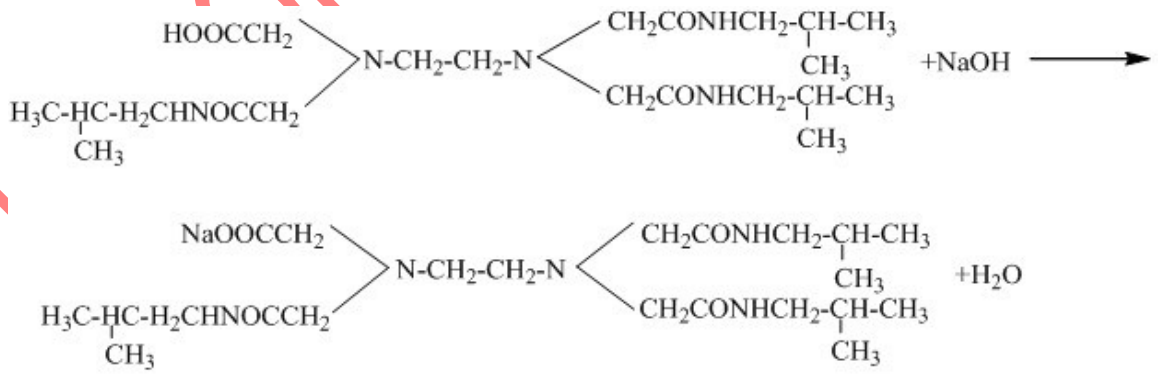

Corrosion and salt precipitation inhibition tests and measurements

Later, the inhibitory properties of the synthesised sodium and potassium salts of mono-, di-, and triisobutylamides of ethylenediaminetetraacetic acid toward corrosion and salt deposition were studied following the methodology described in the article [50], using Steel-3 metal plates (3 cm × 4 cm). To test the corrosion inhibitory properties, two 1000 mL beakers were filled with water from the experimental environment. The water used in the experiment was

slightly alkaline (pH=8.47-8.51), with an electrical conductivity of 598-606 µS/cm and a dissolved oxygen concentration below 5 mg/L. It is similar to those in cooling tower systems. The mineral composition included 53-54 mg/L calcium, 19 mg/L magnesium, and 31-33 mg/L sodium ions. A predetermined amount of the examined salt was added to one of the beakers, and at least two plates were suspended in each beaker. The plates were polished beforehand, wiped with acetone, and dried using filter paper and cotton; their masses were measured with analytical balance, and their surface areas were calculated. Both beakers were placed on magnetic stirrers equipped with heaters and stirred at a speed of 400 rpm. The experiments were conducted at 50°C for 5 hours. The temperature of the water was controlled by a thermometer. The tests were carried out by adding salts to the medium at concentrations of 50, 100 and 150 mg/L. At the end of the experiment, the plates were removed from the water and immersed for one minute in a solution prepared by mixing hydrochloric acid and distilled water in a 1:1 volume ratio, with the addition of 4-6% formalin. The plates were then washed with distilled water, dried, wiped with acetone, and dried again.

After the experiment, the masses of the plates were weighed again on an electronic balance, and the corrosion rates were calculated for both inhibited and uninhibited systems. The mass loss of the metal plates was determined by the formula:

$$\Delta m = m_2 - m_1 \tag{2}$$

where m_1 is the mass of the plate before the experiment and m_2 is the mass after the experiment (Δm was calculated as the average value for the plates). Then the corrosion rates without inhibitor (V_0) and with inhibitor (V_{inh}) were calculated by the equation:

$$V = \frac{\Delta m}{S \times t} \tag{3}$$

where V is the corrosion rate (mg·cm^{-2}·h^{-1}), Δm is the mass loss (mg), S is the surface area of the plate (cm^2), and t is the duration of the experiment (h). Based on the corrosion rate values obtained before (V_o) and after (V_{inh}) the addition of the inhibitor the effectiveness (IE) of the salts as corrosion inhibitors was calculated by the formula:

$$IE = \frac{V_0 - V_{inh}}{V_0} \times 100\% \tag{4}$$

To study the inhibitory properties against salt precipitation, the effectiveness was evaluated based on the difference in the rate of salt precipitation by measuring the concentration of Ca^{2+} ions before and after the experiment in media with and without inhibitors. At this stage, the Ca^{2+} ion concentration was determined by titration using Trilon B. Based on the amount of $CaCO_3$ formed, the rate of salt precipitation was calculated. The efficiency of the samples was determined using the same approach.

As stated in the methodology, the experiments were conducted in several repeated trials. It was ensured that the deviation between the measured values did not exceed 5% for corrosion experiments and 8% for sedimentation experiments, and their average mathematical values were used in the calculations.

Computational calculation method

All Density Functional Theory (DFT) calculations were performed using the ORCA software package [51], [52]. Geometry optimizations were carried out at the B3LYP/6-31G(d) level of theory [53], [54], [55], using the same basis set for all atoms, including the metal ions. Frequency calculations were subsequently performed at the same level of theory on the optimized structures to confirm the nature of the stationary points and to obtain thermodynamic data. The Self-Consistent Field (SCF) convergence criterion was set to TightSCF with a maximum of 125 iterations, and all calculations were run in parallel using 44 processor cores.

Results and discussion

The determined physicochemical properties of the synthesized compounds and the confirmation of their structures by IR spectroscopy are presented. Their corrosion and salt precipitation inhibition properties, as well as adsorption mechanism and theoretical study are also discussed.

Properties and Infrared characterization of the synthesized isobutylamide derivatives of ethylenediaminetetraacetic acid

Aqueous solutions of the sodium and potassium salts of mono-, di-, and triisobutylamides of ethylenediaminetetraacetic acid were prepared at a concentration of 10%, and their main physicochemical properties such as kinematic viscosity at 20°C (ν, mm²/s), density (ρ^{20}, g/cm³), refractive index (n_D^{20}) and freezing point ($T_{freezing}$, °C) were determined. All data are presented in Table 1. The density values ranged from 1.0449 to 1.0484 g/cm³ for the sodium salts and from 1.0400 to 1.0463 g/cm³ for the potassium salts. The kinematic viscosities ranged from 1.3772 to 1.3830 mm²/s for the sodium salts and from 1.5454 to 1.5519 mm²/s for the potassium salts. The lowest freezing point among all the investigated solutions was -5°C.

Table 1. Physicochemical characteristics of 10% aqueous solutions of the sodium and potassium salts of isobutylamides of ethylenediaminetetraacetic acid

Salts of isobutylamides of ethylenediaminetetraacetic acid	ρ^{20}, g/sm³	ν, mm²/s	$T_{freezing}$, °C	n_D^{20}
Trisodium salt	1.0484	1.3830	-5	1.3497
Disodium salt	1.0477	1.3775	-4	1.3473
Monosodium salt	1.0449	1.3772	-4	1.3408
Tripotassium salt	1.0463	1.5519	-5	1.3547
Dipotassium salt	1.0401	1.5454	-4	1.3567
Monopotassium salt	1.0400	1.5494	-4	1.3502

IR spectroscopy was used to confirm the structures of the synthesized compounds. The IR spectra were recorded using an ALPHA Fourier-transform infrared spectrometer manufactured by the German company Bruker. Figure 1 presents the IR spectra of the synthesized sodium and potassium salts of mono- and tri-isobutylamides of ethylenediaminetetraacetic acid. The assignments of the observed IR absorption bands are explained in Table 2.

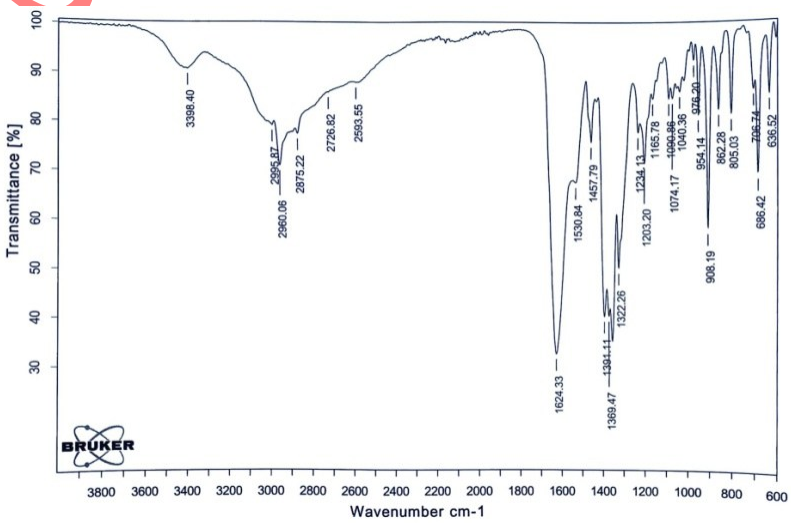

(a)

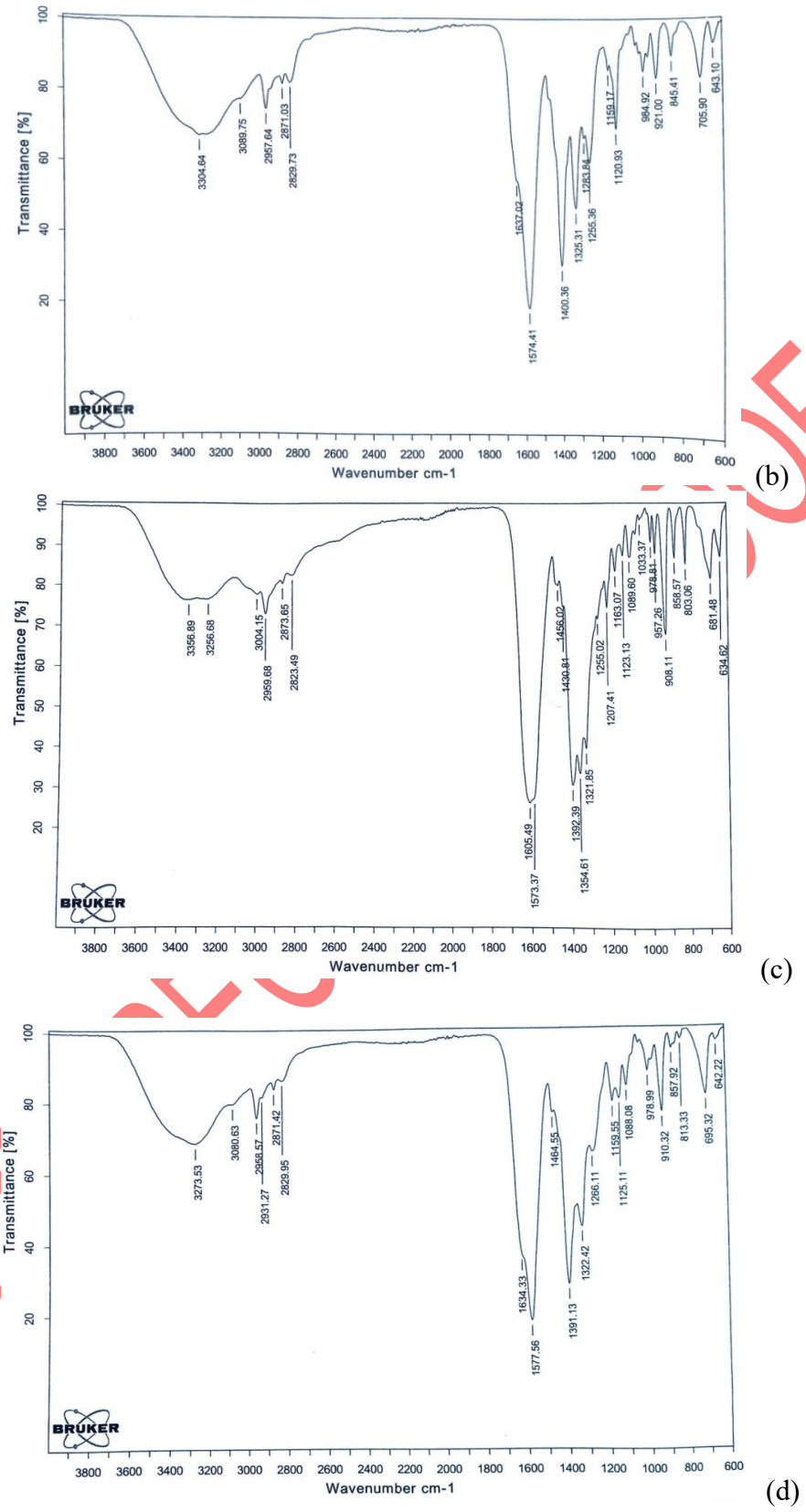

Figure 1. IR spectra of the trisodium (a), monosodium (b), tripotassium (c), and monopotassium (d) salts of isobutylamides of ethylenediaminetetraacetic acid

Table 2. Explanation of the observed spectra of the sodium and potassium salts of mono- and triisobutylamides of ethylenediaminetetraacetic acid

Assignment	Salts of isobutylamides of ethylenediaminetetraacetic acid			
	Trisodium salt	Monosodium salt	Tripotassium salt	Monopotassium salt
	Wavenumber (cm^{-1})			
Deformation vibrations of the $C-H$ and $N-H$ bonds	636, 686, 706, 805, 862, 908, 954, 976	643, 705, 845, 921, 984	634, 681, 803, 858, 908, 957, 978	642, 695, 813, 857, 910, 978
Deformation and valence vibrations of the $C-O$ and $C-N$ bonds	1040, 1074, 1090, 1165, 1203, 1234	1120, 1159, 1255, 1283	1089, 1123, 1163, 1207, 1255	1088, 1125, 1159, 1266
Deformation and valence vibrations of the $C-H$ bond	1322, 2875, 2960	1325, 2829, 2871, 2957	1321, 1354, 2823, 2873, 2959	1322, 2829, 2871, 2958
Carboxylate band	1391	1400	1392	1391
Amide band	1530, 1624	1574, 1637	1573, 1605	1577, 1634
Valence oscillation of the $N-H$ bond	3398	3304	3256, 3356	3080, 3273

As can be seen from the spectra and their interpretations given in the table, absorption bands characteristic of amide and carboxylate groups are observed in the structures of the compounds. These bands correspond to the stretching vibrations of the amide $C=O$ bonds at 1624 cm^{-1} (a), 1637 cm^{-1} (b), 1605 cm^{-1} (c), and 1634 cm^{-1} (d), as well as to the deformation vibrations of the amide $N-H$ bonds at 1530 cm^{-1} (a), 1574 cm^{-1} (b), 1573 cm^{-1} (c), and 1577 cm^{-1} (d). The absorption bands attributed to the symmetric stretching vibration of the carboxylate group were identified at 1391 cm^{-1} (a), 1400 cm^{-1} (b), 1392 cm^{-1} (c), and 1391 cm^{-1} (d). At the same time, it should be noted that the second absorption band of the carboxylate group, which is expected to appear in the 1550-1650 cm^{-1} region of the spectra, overlaps with the absorption bands of the amide groups. Additionally, the absence of a band near 1720 cm^{-1} indicates the complete conversion of carboxylic acid groups to the sodium salt form. The interpretation of the spectra confirms that amide groups were formed during the aminolysis process and that, upon treatment with an alkali to obtain their salts, the carboxyl groups were converted into carboxylate groups.

Inhibition efficiency, adsorption isotherm and mechanism of the synthesized compounds

The results of the experiments conducted to evaluate the effectiveness of the sodium and potassium salts of mono-, di-, and triisobutylamides of ethylenediaminetetraacetic acid against corrosion and salt deposition are given in Table 3.

As shown in Table 3, the corrosion protection efficiency of the sodium and potassium salts of mono-, di-, and triisobutylamides of ethylenediaminetetraacetic acid at concentrations of 50, 100 and 150 mg/L exceeded 70%. At a concentration of 50 mg/L, the highest efficiency (90%) was exhibited by the trisodium salt of monoisobutylamide of ethylenediaminetetracetic acid, whereas the lowest efficiency (70%) was observed for the monopotassium salt. Their inhibitory activity against salt precipitation exceeded 80%, with the trisodium salt again showing the highest efficiency (90%) and the monopotassium salt the lowest (80%) at the same concentration of 50 mg/L. Considering that the inhibition efficiencies of the sodium and potassium salts of mono-, di-, and triisobutylamides of ethylenediaminetetraacetic acid at concentrations of 50, 100, and 150 mg/L exceed 70% for corrosion and 80% for salt deposition, it can be concluded that these compounds exhibit quite high effectiveness.

Table 3. Corrosion and salt deposition inhibitory properties of the sodium and potassium salts of mono-, di-, and triisobutylamides of ethylenediaminetetraacetic acid

Salt	Salt concentration, mg/L	Effectiveness, %	
		Anti-corrosion	Against salt deposition
Trisodium salt of monoisobutylamide of EDTA	50	90	90
	100	96	96
	150	99	98
Disodium salt of diisobutylamide of EDTA	50	88	85
	100	95	92
	150	98	94
Monosodium salt of triisobutylamide of EDTA	50	87	82
	100	94	89
	150	97	93
Tripotassium salt of monoisobutylamide of EDTA	50	74	84
	100	79	88
	150	83	90
Dipotassium salt of diisobutylamide of EDTA	50	72	82
	100	78	85
	150	82	89
Monopotassium salt of triisobutylamide of EDTA	50	70	80
	100	73	81
	150	80	88

The highest result showed trisodium salt of monoisobutylamide of ethylenediaminetetraacetic acid at concentration of 50 mg/L, in case of using at concentrations of 100 and 150 mg/L demonstrated 96% and 99% effectiveness against corrosion, and 96% and 98% effectiveness against salt precipitation, respectively. It should be noted that when sodium and potassium salts of mono-, di-, and triisobutylamides of ethylenediaminetetraacetic acid were used at concentrations of 100 and 150 mg/L, their performance in both corrosion inhibition and anti-scaling activity was higher. As shown in the graphical representations in Figure 2, an increase in effectiveness was observed with increasing concentration.

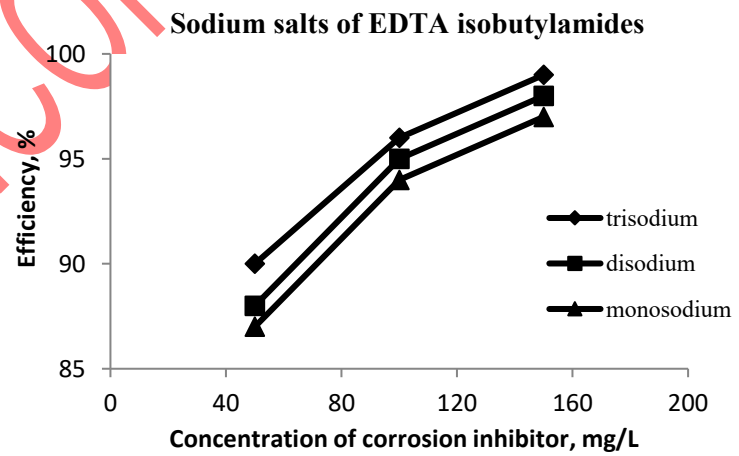

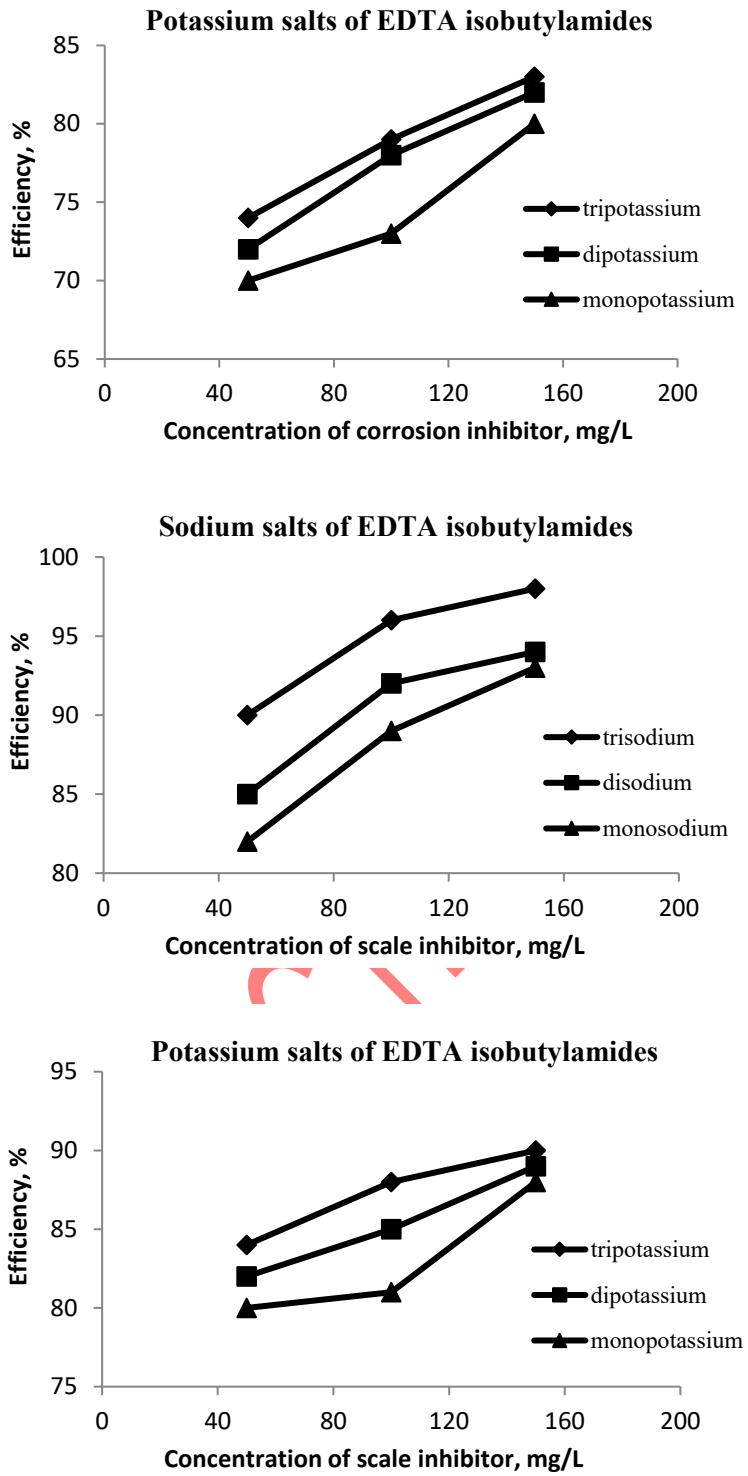

Figure 2. Concentration dependence of the corrosion and salt precipitation inhibitory properties of the sodium and potassium salts of mono-, di-, and triisobutylamides of ethylenediaminetetraacetic acid

It was determined that, overall, among the synthesized salts, the isobutylamides of ethylenediaminetetraacetic acid in the form of trisodium and tripotassium salts exhibit the highest effectiveness against corrosion and salt precipitation. Since the number of anionic groups adsorbed on the surface is higher in the trisodium and tripotassium salts, they provide greater surface coverage and stronger adsorption, forming a more effective coating compared with mono- or disubstituted salts. This, in turn, provides better protection against corrosion and reduces salt precipitation [56], [57]. At the same time, the results indicate that a higher number of anionic groups in the molecule enhances the inhibition of salt precipitation by forming

coordination complexes with the cations responsible for scale deposition, thereby reducing their free concentration in solution and preventing their precipitation as insoluble salts [58], [59]. The order of activity as corrosion and salt precipitation inhibitor for both sodium and potassium salts was found to be mono-<di-<tri-.

The results also showed that mono-, di- and trisodium salts of isobutylamides of ethylenediaminetetraacetic acid are more effective as corrosion inhibitors than the corresponding potassium salts. The higher effectiveness of sodium salts compared with the corresponding potassium salts can be attributed to differences in ion size, hydration, and adsorption behaviour. Sodium ions, being smaller and more strongly hydrated than potassium ions, exhibit stronger salvation in aqueous solutions, which promotes better dissociation of sodium salts and facilitates the release of free anions [60], [61]. Thereby, a more uniform distribution and stronger adsorption of the inhibitor anions on the metal surface are achieved.

As is known, the inhibition efficiency directly depends on the surface covered by adsorbed inhibitor molecules. The degree of surface coverage (θ) can be calculated using corrosion rate values obtained from weight loss measurements at 323 K, according to the following equation:

$$\theta = 1 - \frac{V_{inh}}{V_0} \quad (5)$$

where V_0 and V_{inh} represent the corrosion rates (mg·cm^{-2}·h^{-1}) in the absence and presence of the inhibitor, respectively.

The obtained data are summarized in Table 4. The results indicate that increasing the inhibitor concentration leads to an increase in surface coverage and a corresponding decrease in the corrosion rate. The high surface coverage (θ) value, close to unity, indicates nearly complete coverage of the investigated metal surface by adsorbed molecules. Thus, the surface is efficiently isolated from the corrosive medium. In the absence of the inhibitor, the corrosion rate was found to be 0.59 mg·cm^{-2}·h^{-1}.

Table 4. Corrosion rate and surface coverage data obtained from weight loss measurements for Steel-3 metal plates in the absence and presence of the sodium and potassium salts of mono-, di-, and triisobutylamides of ethylenediaminetetraacetic acid

Salt	Salt concentration, mg/L	Corrosion rate, mg·cm^{-2}·h^{-1}	Surface coverage
Trisodium salt of monoisobutylamide of EDTA	50	0.0573	0.90
	100	0.0231	0.96
	150	0.0118	0.98
Disodium salt of diisobutylamide of EDTA	50	0.0884	0.85
	100	0.0468	0.92
	150	0.0353	0.94
Monosodium salt of triisobutylamide of EDTA	50	0.1056	0.82
	100	0.0642	0.89
	150	0.0411	0.93
Tripotassium salt of monoisobutylamide of EDTA	50	0.0941	0.84
	100	0.0703	0.88
	150	0.0575	0.90
Dipotassium salt of diisobutylamide of EDTA	50	0.1055	0.82
	100	0.0883	0.85
	150	0.0648	0.89
Monopotassium salt of triisobutylamide of EDTA	50	0.118	0.80
	100	0.1118	0.81
	150	0.0706	0.88

Fundamental insights into the interaction between inhibitor molecules and metal surfaces can be received through the analysis of adsorption isotherms. To establish the adsorption isotherm, the degree of surface coverage as a function of inhibitor concentration must be obtained. The applicability of the Langmuir adsorption isotherm was evaluated for its fit to the experimental data of the correlation between the degree of surface coverage and the inhibitor concentration (C_{inh}) in the corrosive medium. The Langmuir isotherm is expressed as follows:

$$\frac{C_{inh}}{\theta} = C_{inh} + \frac{1}{K_{ads}} \quad (6)$$

where C_{inh} is the molar concentration of the inhibitor and K_{ads} is the equilibrium constant of the inhibitor adsorption process.

When a graph of C_{inh}/θ versus C_{inh} was plotted, a straight line with linear correlation coefficients (R^2) close to unity was obtained, as shown in Figure 3. This indicates that the adsorption of the investigated inhibitors on the metal surface at 323 K follows the Langmuir adsorption isotherm model. The corresponding linear regression coefficients are also presented in Figure 3.

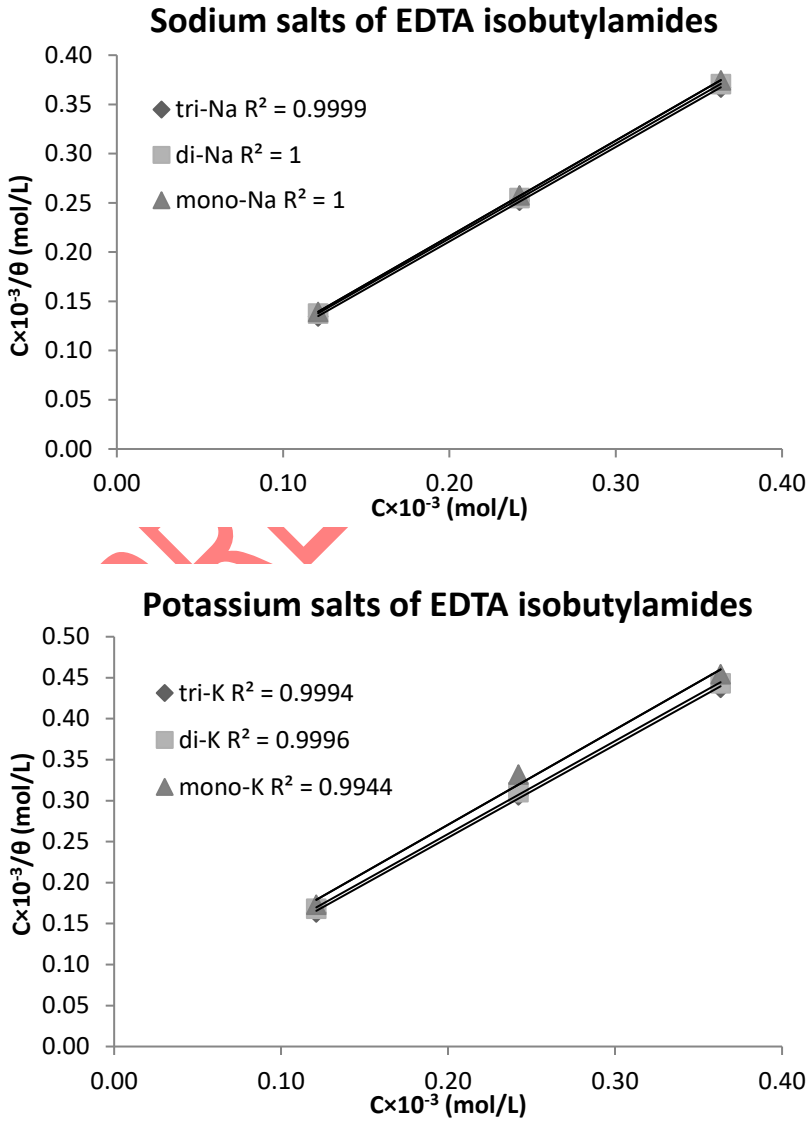

Figure 3. Langmuir adsorption isotherm plots for the sodium and potassium salts of mono-, di-, and triisobutylamides of ethylenediaminetetraacetic acid

The reciprocal intercept values of the Langmuir plots are equal to the adsorption equilibrium constant (K_{ads}), which represents the degree of adsorption and is related to the standard free energy of adsorption (ΔG^o_{ads}) through the following expression:

$$K_{ads} = \frac{1}{55.5}\, exp(-\frac{\Delta G^0_{ads}}{RT}) \quad (7)$$

where ΔG^o_{ads} is the change in Gibbs free energy, K_{ads} is the adsorption equilibrium constant, R is the universal gas constant (8.314 J·K^{-1}·mol^{-1}), T is the absolute temperature and 55.5 is the concentration of water (mol/L).

The values of K_{ads} were used to calculate the standard free energy of adsorption, which characterizes the interaction of inhibitor molecules with the metal surface, and the results are presented in Table 5. The relatively high values of the adsorption equilibrium constant reflect the strong adsorption ability of these salts on the metal surface.

Table 5. Thermodynamic parameters for the adsorption of the sodium and potassium salts of mono-, di-, and triisobutylamides of ethylenediaminetetraacetic acid

Salts of isobutylamides of ethylenediaminetetraacetic acid	K_{ads}, M^{-1}×10^4	ΔG^o_{ads}, kJ·mol^{-1}
Trisodium salt	5.291	-39.99
Disodium salt	4.695	-39.67
Monosodium salt	4.587	-39.61
Tripotassium salt	3.497	-38.88
Dipotassium salt	3.086	-38.55
Monopotassium salt	2.597	-38.08

The mechanism of corrosion inhibition may be explained on the basis of the adsorption behavior of the compounds. The adsorption of corrosion inhibitors on metal surfaces involves two principal types of interactions responsible for the binding process. The first, physical adsorption (physisorption), is characterized by weak, non-directional interactions arising from electrostatic attraction between charged inhibitor species or dipolar molecules and the electrically charged metal surface. The second, chemical adsorption (chemisorption), occurs through stronger, directional interactions, in which charge sharing or charge transfer takes place between the inhibitor molecules and metal surface atoms, leading to the formation of coordinate bonds.

Based on the obtained values of ΔG^o_{ads}, it is possible to predict the adsorption mechanism of the inhibitor molecules on the metal surface. In comparison with physisorption, chemisorption is associated with higher adsorption free energy and activation energy and is therefore generally considered irreversible. Typically, ΔG^o_{ads} values around -20 kJ/mol or less negative are characteristic of physisorption, whereas values around -40 kJ/mol or more negative indicate chemisorption.

The high negative values of ΔG^o_{ads} (Table 5) obtained for the synthesized molecules indicate the spontaneous nature of the adsorption process and the stability of the adsorbed layer on the metal surface, suggesting that adsorption occurs via a chemisorption mechanism. Chemisorption occurs through the adsorption of inhibitor molecules via their functional groups onto the metal surface, involving interactions between the d-orbitals of iron atoms and the lone electron pairs on the sp^2-hybridized nitrogen and oxygen atoms of the inhibitor.

This is because the interaction energy between the inhibitor molecules and the metal surface is higher than that between water molecules and the metal surface, leading to the displacement of water molecules from the surface. Adsorption of inhibitor molecules from an aqueous solution can be regarded as a quasi-substitution process between inhibitor species in the solution and water molecules adsorbed on the metal surface. Consequently, the protective action of the studied inhibitors during metal corrosion is based on their adsorption ability,

whereby the resulting adsorbed film isolates the metal surface from the corrosive medium. Overall, the inhibition efficiency of these compounds is influenced by several factors, including the number and charge density of adsorption active centers, molecular size, and the nature of the interaction between the inhibitor molecules and the metal surface.

Theoretical study

In recent years, atomistic simulations have emerged as a unique and powerful computational tool for advancing corrosion inhibition research [62]. Density Functional Theory is now extensively utilized to establish the correlation between the molecular structure and inhibition performance, providing a theoretical foundation for experimental observations in aggressive environments such as desalination plants [59], [63]. By calculating critical quantum chemical parameters - including frontier molecular orbital distributions and the fraction of electron transfer - researchers can elucidate the specific interaction mechanisms of inhibitors at the metal-electrolyte interface [64], [65]. This computational approach is particularly vital for evaluating multifunctional reagents like EDTA derivatives, as it confirms the role of nucleophilic centers in achieving high protection efficiencies [66].

To provide a theoretical foundation for the experimental observations and to elucidate the structure-activity relationship of the synthesized compounds, DFT calculations were conducted. The primary objective was to investigate the electronic properties and optimized molecular geometries of the inhibitors to understand how their spatial arrangement and functional group distribution influence the interaction with the metal surface. The optimized geometries of the trisodium, monosodium, and tripotassium salts are illustrated in Figure 4.

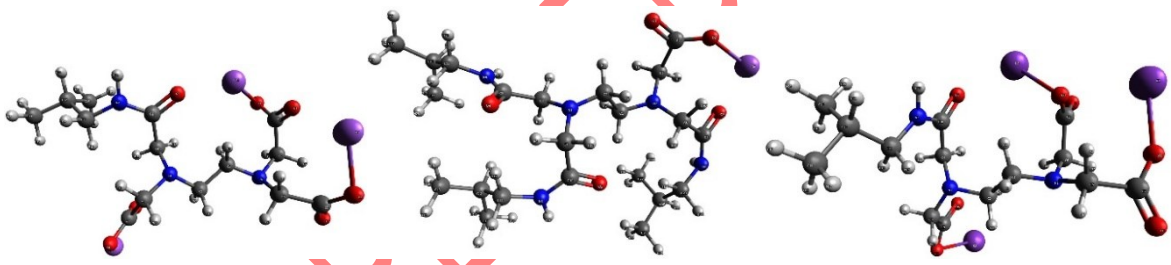

Tri-Na salt **Mono-Na salt** **Tri-K salt**

Figure 4. Optimized molecular structures of the trisodium salt, monosodium salt, and tripotassium salt of isobutylamides of ethylenediaminetetraacetic acid

The optimized structures reveal that the carboxylate groups ($-COO^-$) and the amide linkages ($-\mathrm{CONH}-$) act as the primary nucleophilic centers for coordination with the Steel-3 surface. The $C-O$ bond lengths in the carboxylate groups (ranging from 1.23 to 1.28 Å) and the $C=O$ bonds in the amide groups confirm that these sites are rich in electron density, facilitating the formation of protective layers through chemisorption, as established by the Langmuir isotherm. Similar to findings in existing literature for EDTA analogues [47], the "tri-" substituted salts (trisodium and tripotassium) exhibit a more extended and planar spatial configuration due to the presence of three anionic carboxylate groups. This configuration allows the molecule to occupy a larger surface area on the metal substrate, leading to the higher surface coverage (θ) observed in the corrosion experiments. In contrast, the monosodium salt adopts a more "curled" geometry, which effectively reduces its adsorption footprint and explains its lower efficiency (70-80%) compared to the trisodium salt (90-99%). The calculated bond lengths between the alkali metal ions and the oxygen atoms (approximately 2.10–2.17 Å for $Na-O$ and 2.40–2.65 Å for $K-O$) correlate with the experimental finding that sodium salts outperform potassium salts. The shorter and more specific coordination in the sodium derivatives, combined with their smaller ionic radius and stronger hydration, facilitates

a more uniform dissociation and distribution of the inhibitor anions at the metal-water interface.

Furthermore, to evaluate the electronic interactions and identify the specific sites responsible for electron exchange with the metal surface, the frontier molecular orbital distributions were analyzed (Figure 5).

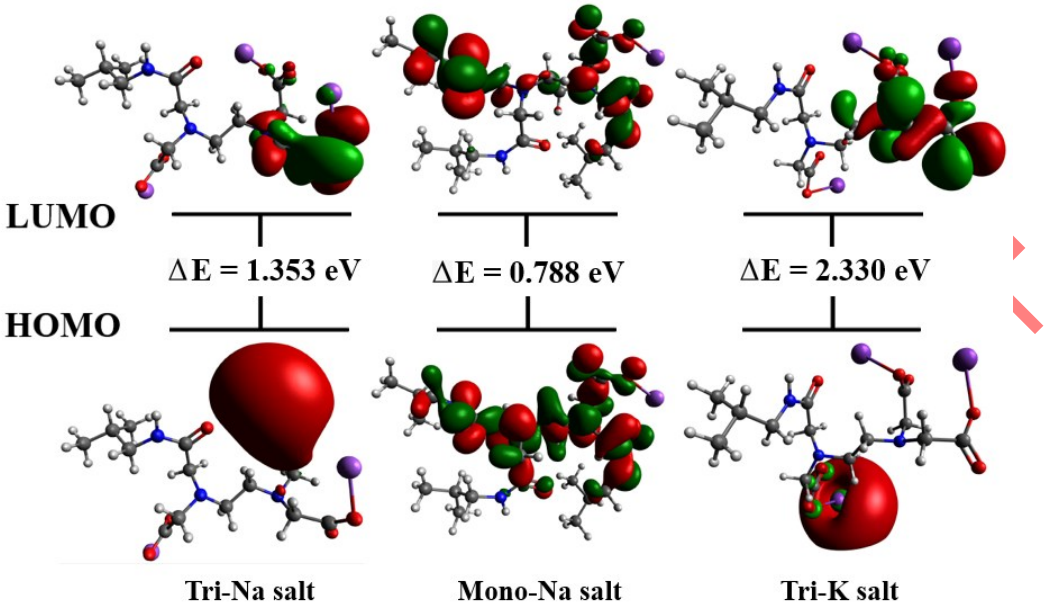

Figure 5. Spatial distribution of HOMO and LUMO density for the optimized structures of the trisodium salt, monosodium salt, and tripotassium salt of isobutylamides of ethylenediaminetetraacetic acid

As shown in Figure 5, the highest occupied molecular orbital (HOMO) density is primarily localized over the carboxylate groups ($-COO^-$) and the nitrogen atoms of the ethylenediamine core. This localization confirms that these regions are the primary nucleophilic centers responsible for donating electrons to the vacant d-orbitals of the iron atoms on the Steel-3 surface. The concentration of HOMO density on the three carboxylate groups in the trisodium and tripotassium salts supports their superior performance, as they offer more "anchoring points" for chemical interaction compared to the monosodium salt. The lowest unoccupied molecular orbital (LUMO) density is largely distributed across the amide linkages ($-\mathrm{CONH}-$) and the carbonyl oxygens. This distribution suggests that these groups can accept back-donated electrons from the metal surface, strengthening the adsorption bond through a synergic mechanism. The broad spatial distribution of both HOMO and LUMO across the entire molecular framework in the trisodium salt indicates a high chemical reactivity and a strong tendency to form a stable, flat-oriented protective film. This molecular "footprint" aligns with the experimental observation that trisodium achieves 99% protection efficiency, as the orbital overlap with the metal surface is maximized in this configuration. The localization of electron density on the carboxylate oxygens also explains the high scale-prevention efficiency (90-98%). These electron-rich regions act as effective chelating sites for Ca^{2+} ions, preventing their precipitation as scale.

In addition to the visual analysis of orbital distributions, several global quantum chemical parameters were calculated to quantitatively assess the reactivity and stability of the inhibitors. These parameters, including ionization potential, electron affinity, electronegativity, chemical hardness, and the fraction of electrons transferred were determined based on the frontier molecular orbital energies (E_{HOMO} and E_{LUMO}) in accordance with established literature methodologies for corrosion inhibition studies [67], [68], [69].

The calculated quantum chemical parameters presented in Table 6 provide a robust theoretical framework for understanding the high inhibition efficiencies observed in the

experimental trials. According to the Frontier Molecular Orbital theory, the interaction between the inhibitor and the metal surface is governed by the energy levels of the HOMO and LUMO. To calculate the fraction of electrons transferred (ΔN), the theoretical values for the absolute electronegativity and chemical hardness of bulk iron were utilized. Following the established literature for corrosion studies on steel, the electronegativity of iron was taken as $\chi \mathrm{Fe} = 7.0$ eV and the chemical hardness as $\eta \mathrm{Fe} = 0$ eV, assuming that the metal surface acts as a soft soft-acid sea of electrons [70]. These reference values allow for a direct quantitative assessment of the electron-donating capability of the synthesized inhibitors toward the Steel-3 substrate.

Table 6. Calculated quantum chemical parameters for the optimized structures of the tri-sodium salt, mono-sodium salt, and tri-potassium salt of isobutylamides of ethylenediaminetetraacetic acid

Parameters	Salts of isobutylamides of ethylenediaminetetraacetic acid		
	trisodium salt	monosodium salt	tripotassium salt
E_{HOMO}	-3.817	-5.140	-3.612
E_{LUMO}	-2.464	-4.352	-1.282
Energy Gap (E_{gap})	1.353	0.788	2.330
Ionization Potential (I)	3.817	5.140	3.612
Electron Affinity (A)	2.464	4.352	1.282
Electronegativity (χ)	3.141	4.746	2.447
Chemical Potential (μ)	-3.141	-4.746	-2.447
Chemical Hardness (η)	0.677	0.394	1.165
Chemical Softness (σ)	0.739	1.269	0.429
Electrophilicity Index (ω)	7.287	28.586	2.570
Fraction of electrons transferred (ΔN)	2.850	2.860	1.954

The fraction of electrons transferred is a critical indicator of the chemical adsorption strength. The calculated ΔN values for all studied inhibitors are positive, confirming that the inhibition mechanism involves the donation of electrons from the inhibitor's active centers (carboxylate and amide groups) to the vacant d-orbitals of the iron atoms. Notably, the ΔN values for the sodium salts (trisodium: 2.850; monosodium: 2.860) are significantly higher than that of the potassium salt (tripotassium: 1.954). This theoretical finding perfectly supports the experimental evidence that sodium-based derivatives provide superior corrosion protection. According to the Hard-Soft Acid-Base principle, "soft" molecules (lower η) are more reactive and tend to form stronger coordinate bonds with metal surfaces. The trisodium salt exhibits a lower chemical hardness (0.677 eV) compared to the tripotassium salt (1.165 eV), indicating that the sodium derivative is more polarizable and can more effectively interact with the Steel-3 surface to form a stable protective film.

The energy gap ($E_{LUMO} - E_{HOMO}$) is an indicator of the kinetic stability and reactivity of the molecule. The relatively low energy gaps for the trisodium and monosodium salts suggest higher reactivity at the metal-electrolyte interface, which aligns with the rapid formation of the protective layer observed in the weight-loss and scale-prevention tests. The absolute electronegativity values reflect the tendency of the molecules to attract electrons. The balance between χ and η in the trisodium salt optimizes its role as an electron donor, consistent with the 99% inhibition efficiency and 98% scale prevention measured at 150 mg/L [70], [71], [72].

By aligning these quantum chemical parameters with the experimental data, it is evident that the trisodium salt of EDTA isobutylamide possesses the most favorable electronic profile for multifunctional protection. The higher electron-transfer capability and lower molecular hardness of the sodium derivatives explain their dominant performance over the potassium-based analogues in 50°C aqueous environments.

Conclusions

The sodium and potassium salts of isobutylamides of ethylenediaminetetraacetic acid were synthesized, their structures were confirmed by IR spectroscopy, and their 10% solutions were prepared to determine the main physicochemical properties.

The synthesized salts were tested as corrosion and scale formation inhibitors at 50°C, and it was determined that the sodium salts are more effective than the potassium salts, with their activity ranking in the order of mono- < di- < tri-.

The highest efficiency as a corrosion and salt precipitation inhibitor at a concentration of 50 mg/L was achieved with the trisodium salt of monoisobutylamide of ethylenediaminetetraacetic acid. At this concentration, it protected the Steel-3 metal plate from corrosion by 90%, and its effectiveness against salt deposition was also 90%. The inhibitory properties against corrosion and salt deposition increased when the salt was added to the medium at concentrations of 100 and 150 mg/L. At the same time, it was determined that the effectiveness of all synthesized salts as corrosion and scale inhibitors was directly proportional to their concentration.

The adsorption behaviour of the studied compounds on the steel surface obeyed the Langmuir adsorption isotherm, while the obtained standard free energy of adsorption values confirmed that the mechanism is chemisorption.

Quantum chemical calculations revealed that among the synthesized compounds, the sodium salts - particularly the trisodium salt - exhibited higher electron transfer capabilities ($\Delta N = 2.850$) compared to their potassium analogues. DFT analysis confirmed that the three anionic carboxylate centers in the trisodium salt facilitate a broader spatial configuration and maximized orbital overlap with the metal surface, providing a theoretical basis for its peak protection efficiency of 99%. These theoretical descriptors perfectly align with the experimentally established activity order of mono- < di- < tri-, validating the role of multi-center coordination in enhancing multifunctional inhibition performance.Nomenclature

Symbols

$T_{freezing}$	Freezing point	°C
m_1	Mass of the plate before experiment	[mg]
m_2	Mass of the plate after experiment	[mg]
Δm	Mass loss	[mg]
V	Corrosion rate	$[g \cdot m^{-2} \cdot h^{-1}]$
V_0	Corrosion rate without inhibitor	$[g \cdot m^{-2} \cdot h^{-1}]$
V_{inh}	Corrosion rate in presence of inhibitor	$[g \cdot m^{-2} \cdot h^{-1}]$
S	Surface area	$[cm^2]$
t	Duration	[h]
IE	Effectiveness	[%]
ΔG^0_{ads}	The standard free energy of adsorption	$[kJ \cdot mol^{-1}]$
K_{ads}	The equilibrium constant of the inhibitor adsorption process	$[L \cdot mol^{-1}]$
C_{inh}	Molar concentration of the inhibitor	$[mol \cdot L^{-1}]$
R^2	Correlation coefficient	-
R	Universal gas constant	$[J \cdot K^{-1} \cdot mol^{-1}]$
T	Absolute temperature	[K]
E_{HOMO}	Energy of the highest occupied molecular orbital	eV
E_{LUMO}	Energy of the lowest unoccupied molecular orbital	eV
E_{gap}	Energy gap	eV
I	Ionization potential	eV

A	Electron affinity	eV
ΔN	Fraction of electrons transferred	-

Greek letters

ρ	density	[g/cm³]
n_D^{20}	refractive index	-
v	kinematic viscosity	[mm²/s]
θ	the degree of surface coverage	-
χ	Electronegativity	eV
μ	Chemical potential	eV
η	Chemical hardness	eV
σ	Chemical softness	eV^{-1}
ω	Electrophilicity index	eV

Abbreviations

Steel-3	Low carbon mild steel
EDTA	Ethylenediaminetetraacetic acid
DFT	Density functional theory
SCF	Self consistent field
ORCA	Quantum chemistry program
HOMO	Highest occupied molecular orbital
LUMO	Lowest unoccupied molecular orbital

REFERENCES

[1] K. D. Demadis, E. Mavredaki, A. Stathoulopoulou, E. Neofotistou, and C. Mantzaridis, 'Industrial water systems: problems, challenges and solutions for the process industries', *Desalination*, vol. 213, no. 1–3, pp. 38–46, Jul. 2007, doi: 10.1016/j.desal.2006.01.042.

[2] J. Li, M. Tang, Z. Ye, L. Chen, and Y. Zhou, 'Scale formation and control in oil and gas fields: A review', *Journal of Dispersion Science and Technology*, vol. 38, no. 5, pp. 661–670, May 2017, doi: 10.1080/01932691.2016.1185953.

[3] S. E. Coetser and T. E. Cloete, 'Biofouling and Biocorrosion in Industrial Water Systems', *Critical Reviews in Microbiology*, vol. 31, no. 4, pp. 213–232, Jan. 2005, doi: 10.1080/10408410500304074.

[4] O. S. I. Fayomi, I. G. Akande, and S. Odigie, 'Economic Impact of Corrosion in Oil Sectors and Prevention: An Overview', *J. Phys.: Conf. Ser.*, vol. 1378, no. 2, p. 022037, Dec. 2019, doi: 10.1088/1742-6596/1378/2/022037.

[5] M. M. Vazirian, T. V. J. Charpentier, M. De Oliveira Penna, and A. Neville, 'Surface inorganic scale formation in oil and gas industry: As adhesion and deposition processes', *Journal of Petroleum Science and Engineering*, vol. 137, pp. 22–32, Jan. 2016, doi: 10.1016/j.petrol.2015.11.005.

[6] G. R. Puchina *et al.*, 'Modern practice of salt deposition preventing and removing', *NGD*, vol. 18, no. 2, pp. 72–80, Jun. 2020, doi: 10.17122/ngdelo-2020-2-72-80.

[7] Abbasov V.M. *et al.*, *Reagents and Products for the Oil, Gas, Oil Refining and Petrochemical Industries*. Baku: Elm, 2017.

[8] M. S. Kamal, I. Hussein, M. Mahmoud, A. S. Sultan, and M. A. S. Saad, 'Oilfield scale formation and chemical removal: A review', *Journal of Petroleum Science and Engineering*, vol. 171, pp. 127–139, Dec. 2018, doi: 10.1016/j.petrol.2018.07.037.

[9] R. D. Vidic, W. Liu, H. Li, and C. He, 'Water Treatment Chemicals: Types, solution chemistry, and applications', in *Mineral Scales and Deposits*, Elsevier, 2015, pp. 169–191. doi: 10.1016/B978-0-444-63228-9.00008-5.

[10] V. M. Abbasov *et al.*, 'Applicability of novel anionic surfactant as a corrosion inhibitor of mild steel and for removing thin petroleum films from water surface', *American Journal of Materials Science and Engineering*, vol. 1, no. 2, pp. 18–23, 2013, https://pubs.sciepub.com/ajmse/1/2/1/index.html.

[11] S. Zhang *et al.*, 'Enhanced scale inhibition against $Ca_3(PO_4)_2$ and Fe_2O_3 in water using multi-functional fluorescently-tagged antibacterial scale inhibitors', *Environ. Sci.: Water Res. Technol.*, vol. 6, no. 4, pp. 951–962, 2020, doi: 10.1039/C9EW01036J.

[12] I. T. Ismayilov, 'Synthesis and properties of the multifunctional anticorrosive reagents on the basis of sunflower oil and ethanolamines', *Processes of Petrochemistry and Oil Refining*, vol. 17, no. 4, pp. 331–346, 2016.

[13] Yu. I. Kuznetsov, 'Triazoles as a class of multifunctional corrosion inhibitors. A review. Part I. 1,2,3-Benzotriazole and its derivatives. Copper, zinc and their alloys', *Int. J. Corros. Scale Inhib.*, vol. 7, no. 3, pp. 271–307, Oct. 2018, doi: 10.17675/2305-6894-2018-7-3-1.

[14] Y. Hu, C. Chen, and S. Liu, 'State of art bio-materials as scale inhibitors in recirculating cooling water system: a review article', *Water Science and Technology*, vol. 85, no. 5, pp. 1500–1521, Mar. 2022, doi: 10.2166/wst.2022.027.

[15] N. D. Nabiyeva, *et al.*, 'Study of inhibitory-bactericidal properties of the byproduct of white oil production against deemulsifier and corrosion', *Processes of Petrochemistry and Oil Refining*, vol. 22, no. 4, pp. 546–551, 2021, https://ppor.az/index.php/ppor/article/view/277.

[16] I. T. Ismayilov, *et al.*, 'Enhanced corrosion inhibition of mild steel in CO_2-saturated solutions containing some novel green surfactants based on cottonseed oil', *Int. J. Corros. Scale Inhib.*, vol. 4, no. 1, pp. 057–074, 2015, doi: 10.17675/2305-6894-2015-4-1-057-074.

[17] V. M. Abbasov, I. T. Ismayilov, H. M. Abd El-Lateef, and S. F. Akhmadbeyova, 'Anti-corrosive activities of some novel surfactants based on vegetable oils', *European Chemical Bulletin*, vol. 3, no. 5, pp. 437–440, 2014.

[18] D.-J. Choi, S.-J. You, and J.-G. Kim, 'Development of an environmentally safe corrosion, scale, and microorganism inhibitor for open recirculating cooling systems', *Materials Science and Engineering: A*, vol. 335, no. 1–2, pp. 228–235, Sep. 2002, doi: 10.1016/S0921-5093(01)01928-1.

[19] M. A. Jafar Mazumder, 'A Review of Green Scale Inhibitors: Process, Types, Mechanism and Properties', *Coatings*, vol. 10, no. 10, p. 928, Sep. 2020, doi: 10.3390/coatings10100928.

[20] X. Wang, J. Yang, X. Chen, C. Liu, and J. Zhao, 'Synergistic inhibition properties and microstructures of self-assembled imidazoline and phosphate ester mixture for carbon steel corrosion in the CO_2 brine solution', *Journal of Molecular Liquids*, vol. 357, p. 119140, Jul. 2022, doi: 10.1016/j.molliq.2022.119140.

[21] S. Bahrami, A. E. S. Van Driessche, M. F. Mady, and R. Panahi, 'A Synergistic Approach to Develop Sustainable Scale Inhibitors Combining Amino Acids and Polyphosphates', *Water Air Soil Pollut*, vol. 235, no. 7, p. 456, Jul. 2024, doi: 10.1007/s11270-024-07289-w.

[22] F. Liu *et al.*, 'Optimizations of inhibitors compounding and applied conditions in simulated circulating cooling water system', *Desalination*, vol. 313, pp. 18–27, Mar. 2013, doi: 10.1016/j.desal.2012.11.028.

[23] R. Ketrane, B. Saidani, O. Gil, L. Leleyter, and F. Baraud, 'Efficiency of five scale inhibitors on calcium carbonate precipitation from hard water: Effect of temperature and concentration', *Desalination*, vol. 249, no. 3, pp. 1397–1404, Dec. 2009, doi: 10.1016/j.desal.2009.06.013.

[24] Z. Amjad and K. Demadis, *Water-Formed Deposits: Fundamentals and Mitigation Strategies*. Amsterdam: Elsevier, 2022.

[25] N. A. Karpunin, Ryazanov A.A., Khromyh L.N., and Shukin N.A., 'Modern experience handling bottomhole formation zone of terrigenous deposit by acid compositions', *The Eurasian Scientific Journal*, vol. 4, no. 10, p. 42NZVN418, 2018, https://esj.today/PDF/42NZVN418.pdf.

[26] P. Zhang, D. Shen, G. Ruan, A. T. Kan, and M. B. Tomson, 'Phosphino-polycarboxylic acid modified inhibitor nanomaterial for oilfield scale control: Synthesis, characterization and migration', *Journal of Industrial and Engineering Chemistry*, vol. 45, pp. 366–374, Jan. 2017, doi: 10.1016/j.jiec.2016.10.004.

[27] M. F. Mady, S. Fevang, and M. A. Kelland, 'Study of Novel Aromatic Aminomethylenephosphonates as Oilfield Scale Inhibitors', *Energy Fuels*, vol. 33, no. 1, pp. 228–237, Jan. 2019, doi: 10.1021/acs.energyfuels.8b03531.

[28] I. T. Ismayilov, 'Anti-Corrosion Ability of Some Surfactants Based on Corn Oil and Monoethanolamine', *AJAC*, vol. 1, no. 5, pp. 79–86, 2013, doi: 10.11648/j.ajac.20130105.11.

[29] H. M. Abd El-Lateef, V. M. Abbasov, L. I. Aliyeva, and I. T. Ismayilov, 'Application of Some Surfactants Based on Corn Oil as Corrosion Inhibitors for Carbon Steel in CO_2 Environments', in *CORROSION 2013*, Orlando, FL: NACE International, Mar. 2013, pp. 1–10. doi: 10.5006/C2013-02129.

[30] Z. Shen, J. Li, K. Xu, L. Ding, and H. Ren, 'The effect of synthesized hydrolyzed polymaleic anhydride (HPMA) on the crystal of calcium carbonate', *Desalination*, vol. 284, pp. 238–244, Jan. 2012, doi: 10.1016/j.desal.2011.09.005.

[31] K. Popov, M. Oshchepkov, S. Kamagurov, S. Tkachenko, J. Dikareva, and G. Rudakova, 'Synthesis and properties of novel fluorescent-tagged polyacrylate-based scale inhibitors', *Journal of Applied Polymer Sci*, vol. 134, no. 26, p. app.45017, Jul. 2017, doi: 10.1002/app.45017.

[32] Y. Xiong and M. Cao, 'Application of surfactants in corrosion inhibition of metals', *Current Opinion in Colloid & Interface Science*, vol. 73, p. 101830, Oct. 2024, doi: 10.1016/j.cocis.2024.101830.

[33] Zahraa A. Jawad and Falah K. Matloub, 'Synergistic corrosion inhibition of carbon steel in cooling tower systems using sodium benzoate, zinc sulfate, and EDTA', *Appl. Chem. Eng.*, vol. 8, no. 3, p. 5735, Sep. 2025, doi: 10.59429/ace.v8i3.5735.

[34] A. Shaban *et al.*, 'Synergistic effect of sodium benzoate and EDTA as corrosion inhibitors for carbon steel in chloride-containing solutions', *Corrosion Science*, vol. 125, pp. 61–69, 2017, doi: 10.1016/j.corsci.2017.06.027.

[35] N. Brixi, L. Sail, A. Bezzar, O. Sebouai, and S. Benmesmoudi, 'Temperature Effects on Corrosion Inhibition of Mild Steel in 3% NaCl Solution by EDTA and Sodium Benzoate', in *Proceedings of the Third International Symposium on Materials and Sustainable Development*, B. Abdelbaki, B. Safi, and M. Saidi, Eds, Cham: Springer International Publishing, 2018, pp. 385–397. doi: 10.1007/978-3-319-89707-3_45.

[36] B. S. Bageri, M. A. Mahmoud, R. A. Shawabkeh, S. H. Al-Mutairi, and A. Abdulraheem, 'Toward a complete removal of barite (barium sulfate $BaSO_4$) scale using chelating agents and catalysts', *Arab J Sci Eng*, vol. 42, no. 4, pp. 1667–1674, Apr. 2017, doi: 10.1007/s13369-017-2417-2.

[37] S. Ziegenheim *et al.*, 'EDTA analogues – unconventional inhibitors of gypsum precipitation', *Journal of Molecular Structure*, vol. 1256, p. 132491, May 2022, doi: 10.1016/j.molstruc.2022.132491.

[38] T. Almubarak, J. H. Ng, R. Ramanathan, and H. A. Nasr-El-Din, 'Chelating agents for oilfield stimulation: Lessons learned and future outlook', *Journal of Petroleum Science and Engineering*, vol. 205, p. 108832, Oct. 2021, doi: 10.1016/j.petrol.2021.108832.

[39] A. Khormali and D. G. Petrakov, 'Laboratory investigation of a new scale inhibitor for preventing calcium carbonate precipitation in oil reservoirs and production equipment', *Pet. Sci.*, vol. 13, no. 2, pp. 320–327, May 2016, doi: 10.1007/s12182-016-0085-6.

[40] M. Mpelwa and S.-F. Tang, 'State of the art of synthetic threshold scale inhibitors for mineral scaling in the petroleum industry: a review', *Pet. Sci.*, vol. 16, no. 4, pp. 830–849, Aug. 2019, doi: 10.1007/s12182-019-0299-5.

[41] A. T. Kan, Z. Dai, and M. B. Tomson, 'The state of the art in scale inhibitor squeeze treatment', *Pet. Sci.*, vol. 17, no. 6, pp. 1579–1601, Dec. 2020, doi: 10.1007/s12182-020-00497-z.

[42] M.-L. Zhu, H.-J. Qian, R.-X. Yuan, D.-Y. Zhao, H.-C. Huang, and H.-Y. Wang, 'EDTA interfacial chelation Ca^{2+} incorporates superhydrophobic coating for scaling inhibition of $CaCO_3$ in petroleum industry', *Pet. Sci.*, Feb. 2021, doi: 10.1007/s12182-021-00558-x.

[43] Q. Qu, S. Jiang, W. Bai, and L. Li, 'Effect of ethylenediamine tetraacetic acid disodium on the corrosion of cold rolled steel in the presence of benzotriazole in hydrochloric acid', *Electrochimica Acta*, vol. 52, no. 24, pp. 6811–6820, Aug. 2007, doi: 10.1016/j.electacta.2007.04.114.

[44] L. R. B. Holzle, D. S. Azambuja, C. M. S. Piatnicki, and G. E. Englert, 'Corrosion behaviour of aluminium in ethyleneglycol–water electrolytes containing phosphonic acid', *Materials Chemistry and Physics*, vol. 103, no. 1, pp. 59–64, May 2007, doi: 10.1016/j.matchemphys.2007.01.007.

[45] G. M. Treacy, A. L. Rudd, and C. B. Breslin, 'Electrochemical behaviour of aluminium in the presence of EDTA-containing chloride solutions', *Journal of Applied Electrochemistry*, vol. 30, no. 6, pp. 675–683, Jun. 2000, doi: 10.1023/A:1003945214539.

[46] R. E. Azooz and S. M. Kamal, 'Corrosion and Corrosion Inhibition of Mild Steel in Red Sea Water by EDTA', *Journal of Material Sciences & Engineering*, vol. 8, no. 2, p. 1000517, 2019, https://www.hilarispublisher.com/open-access/corrosion-and-corrosion-inhibition-of-mild-steel-in-red-sea-water-byedta.pdf.

[47] R. E. Azooz, 'EDTA as a corrosion inhibitor for Al in 0.5 M HCl: adsorption, thermodynamic and theoretical study', *J. Electrochem. Sci. Eng.*, vol. 6, no. 3, pp. 235-251, Sep. 2016, doi: 10.5599/jese.300.

[48] T. A. Ismayilov *et al.*, 'Study of salts obtained from the interaction of ethylenediamintetraacetic acid with propylamine and isobutylamine as corrosion inhibitors in H_2S condition', *Processes of Petrochemistry and Oil Refining*, no. Special Issue 1, pp. 156–164, 2024, doi: 10.62972/1726-4685.si2024.1.156.

[49] I. T. Ismayilov, *et al.*, "Investigation of Na^+, K^+ salts of propyl- and isobutylamide derivatives of ethylenediaminetetraacetic acid as biocides in relation to sulfate-reducing bacteria,", *Processes of Petrochemistry and Oil Refining*, vol. 24, no. 3, pp 514–525, 2023, doi: 10.36719/1726-4685/95/514-525.

[50] T. A. Ismailov *et al.*, 'Study of the Na^+ and K^+ salts of ethanolamides of ethylenediaminetetraacetic acid as corrosion and salt precipitation inhibitors', *Processes of Petrochemistry and Oil Refining*, vol. 26, no. 03, p. 917–932, 2025, doi: 10.62972/1726-4685.2025.3.917.

[51] F. Neese, F. Wennmohs, U. Becker, and C. Riplinger, 'The ORCA quantum chemistry program package', *The Journal of Chemical Physics*, vol. 152, no. 22, p. 224108, Jun. 2020, doi: 10.1063/5.0004608.

[52] F. Neese, 'Software Update: The ORCA Program System—Version 6.0', *WIREs Comput Mol Sci*, vol. 15, no. 2, p. e70019, Mar. 2025, doi: 10.1002/wcms.70019.

[53] C. Lee, W. Yang, and R. G. Parr, 'Development of the Colle-Salvetti correlation-energy formula into a functional of the electron density', *Phys. Rev. B*, vol. 37, no. 2, pp. 785–789, Jan. 1988, doi: 10.1103/PhysRevB.37.785.

[54] A. D. Becke, 'Density-functional thermochemistry. III. The role of exact exchange', *The Journal of Chemical Physics*, vol. 98, no. 7, pp. 5648–5652, Apr. 1993, doi: 10.1063/1.464913.

[55] G. A. Petersson and M. A. Al-Laham, 'A complete basis set model chemistry. II. Open-shell systems and the total energies of the first-row atoms', *The Journal of Chemical Physics*, vol. 94, no. 9, pp. 6081–6090, May 1991, doi: 10.1063/1.460447.

[56] E. D. Akpan *et al.*, 'Coordination compounds as corrosion inhibitors of metals: A review', *Coordination Chemistry Reviews*, vol. 499, p. 215503, Jan. 2024, doi: 10.1016/j.ccr.2023.215503.

[57] I. Azamian, S. R. Allahkaram, M. Johari, and F. Teymouri, 'Interfacial interaction study of EDTA with the defect structure of $Fe_{3-\delta}O_4$ passive film in an aggressive alkaline medium based on the lattice theory of point defects', *RSC Adv.*, vol. 12, no. 6, pp. 3524–3541, 2022, doi: 10.1039/D1RA07171H.

[58] X. Li, J. Zhang, J. Zhang, D. Li, S. Chang, and Z. Lei, 'Study on the scale inhibition performance of organic chelating agent aided by surfactants on $CaCO_3$ at high salinity condition', *Tenside Surfactants Detergents*, vol. 61, no. 2, pp. 170–178, Mar. 2024, doi: 10.1515/tsd-2023-2549.

[59] A. M. Al-Sabagh, N. M. El Basiony, S. A. Sadeek, and M. A. Migahed, 'Scale and corrosion inhibition performance of the newly synthesized anionic surfactant in desalination plants: Experimental, and theoretical investigations', *Desalination*, vol. 437, pp. 45–58, Jul. 2018, doi: 10.1016/j.desal.2018.01.036.

[60] T. A. Ismayilov, V. M. Abbasov, I. T. Ismayilov, R. M. Farhadova, E. A. Manafov, and Ch. K. Salmanova, 'Effectiveness of propylamide derivatives of ethylenediaminetetraacetic acid against corrosion and salt deposition problems', *SOCAR Proceedings*, no. 4, pp. 158–166, 2025, doi: 10.5510/OGP20250401135.

[61] E. Udabe, A. Sommers, M. Forsyth, and D. Mecerreyes, 'Cation Effect in the Corrosion Inhibition Properties of Coumarate Ionic Liquids and Acrylic UV-Coatings', *Polymers*, vol. 12, no. 11, p. 2611, Nov. 2020, doi: 10.3390/polym12112611.

[62] I. B. Obot, K. Haruna, and T. A. Saleh, 'Atomistic Simulation: A Unique and Powerful Computational Tool for Corrosion Inhibition Research', *Arab J Sci Eng*, vol. 44, no. 1, pp. 1–32, Jan. 2019, doi: 10.1007/s13369-018-3605-4.

[63] H. Balasooriya, C. Li, and F. Wang, 'Understanding Steel Corrosion: Surface Chemistry and Defects Explored Through DFT Modelling—A Review', *Processes*, vol. 13, no. 7, p. 1971, Jun. 2025, doi: 10.3390/pr13071971.

[64] H. Lgaz, A. Chaouiki, R. Lamouri, R. Salghi, and H.-S. Lee, 'Computational Methods of Corrosion Inhibition Assessment', in *ACS Symposium Series*, vol. 1403, C. M. Hussain and C. Verma, Eds. Washington, DC: American Chemical Society, 2021, pp. 87–109. doi: 10.1021/bk-2021-1403.ch006.

[65] J. M. Castillo-Robles, E. De Freitas Martins, P. Ordejón, and I. Cole, 'Molecular modeling applied to corrosion inhibition: a critical review', *npj Mater Degrad*, vol. 8, no. 1, p. 72, Jul. 2024, doi: 10.1038/s41529-024-00478-2.

[66] S. J. H. M. Jessima, S. S., A. Berisha, A. Oral, and S. S. Srikandan, 'Corrosion mitigation performance of disodium EDTA functionalized chitosan biomacromolecule - Experimental and theoretical approach', *International Journal of Biological Macromolecules*, vol. 178, pp. 477–491, May 2021, doi: 10.1016/j.ijbiomac.2021.02.166.

[67] I. Lukovts, E. Kálmán, and F. Zucchi, 'Corrosion Inhibitors—Correlation Between Electronic Structure and Efficiency', *Corrosion*, vol. 57, no. 1, pp. 3–8, Jan. 2001, doi: 10.5006/1.3290328.

[68] H. Ju, L. Ding, C. Sun, and J. Chen, 'Quantum Chemical Study on the Corrosion Inhibition of Some Oxadiazoles', *Advances in Materials Science and Engineering*, p. 519606, 2015, doi: 10.1155/2015/519606.

[69] N. S. Orujova *et al.*, 'In vitro, in silico, and DFT evaluation of antimicrobial imidazole derivatives with insights into mechanism of action', *Sci Rep*, vol. 15, no. 1, p. 37723, Oct. 2025, doi: 10.1038/s41598-025-24847-2.

[70] M. A. A. Ibrahim *et al.*, 'Density functional theory study of the corrosion inhibition performance of 6-mercaptopurine and 6-thioguanine expired drugs toward the aluminium (111) surface', *RSC Adv.*, vol. 13, no. 41, pp. 29023–29034, 2023, doi: 10.1039/D3RA04954J.

[71] H. M. Abd El-Lateef, V. M. Abbasov, L. I. Aliyeva, E. E. Qasimov, and I. T. Ismayilov, 'Inhibition of carbon steel corrosion in CO_2-saturated brine using some newly surfactants based on palm oil: Experimental and theoretical investigations', *Materials Chemistry and Physics*, vol. 142, no. 2–3, pp. 502–512, Nov. 2013, doi: 10.1016/j.matchemphys.2013.07.044.

[72] A. M. Mammadov *et al.*, 'Inhibitory-Bactericidal Properties of Phenyldiazenylphenyl-Containing Phenanthroimidazoles and DFT Calculations', *Bulletin of the Russian Academy of Sciences: Physics*, vol. 89, no. 9, pp. 1619–1625, Sep. 2025, doi: 10.1134/S1062873825712322.